Tracking the Best Beam for a Mobile User via Bayesian Optimization

Lorenzo Maggi, Ryo Koblitz, Qiping Zhu, Matthew Andrews

Nokia

Abstract—The standard beam management procedure in 5G requires the user equipment (UE) to periodically measure the received signal reference power (RSRP) on each of a set of beams proposed by the basestation (BS). It is prohibitively expensive to measure the RSRP on all beams and so the BS should propose a beamset that is large enough to allow a high-RSRP beam to be identified, but small enough to prevent excessive reporting overhead. Moreover, the beamset should evolve over time according to UE mobility. We address this fundamental performance/overhead trade-off via a Bayesian optimization technique that requires no or little training on historical data and is rooted on a low complexity algorithm for the beamset choice with theoretical guarantees. We show the benefits of our approach on 3GPP compliant simulation scenarios.

Index Terms—Beamforming, RSRP, Bayesian optimization, beam tracking, overhead reduction

I. Introduction

Millimeter-wave (mmWave) frequencies are attractive for next-generation wireless networks due to the large amount of bandwidth available. One challenge with mmWave frequencies is the high penetration loss but this can be mitigated by the gains achievable with large antenna arrays [1]. At high frequencies, antenna spacing can be smaller thus more antennas can be packed into a specified space, which in turn lets us use more directive beams to compensate for the penetration loss. However, with a large antenna array it is prohibitively expensive to have a separate radio chain controlling each antenna. A common solution is the *hybrid beamforming* (HBF) architecture [2] where analogue beams are created by phase-shifters and digital precoding is performed on a set of radio chains that is smaller than the total number of antennas.

In mmWave band 5G systems, the beam management is usually based on the analogue beam domain and the system is designed to be compatible with a hierarchical beam searching structure [3]. In initial access (IA), the synchronized signal block (SSB) can be transmitted with wide beams while in data transmission, the channel state information reference signal (CSI-RS) can be transmitted through refined beams with the mainlobe contained within the selected wide beam from IA.

The base station (BS) will sweep all the possible wide beams periodically for IA, and it may also sweep all the possible refined beams periodically for high refined beam gain tracking if it is serving a large number of users. Each user equipment (UE) measures a *subset* of the beams and reports back to the BS the *Received Signal Reference Power* (RSRP)

for each beam in the subset. From these measurements the BS selects the "best" beam for the UE. We stress that this architecture does not require any channel estimation, which becomes a challenge as the number of antennas grows large.

After the analogue beam selection is complete, the BS then performs scheduling, i.e., it chooses a set of UEs to receive data. Lastly, digital precoding is performed by the radio chains to minimize the interference across UEs.

In this work we focus on the selection of the analogue beams for the downlink for which a specific UE must report RSRP measurements to the BS. Our scheme can be applied to both SSB and CSI-RS beams and so in the sequel we do not make a distinction. The goal is to choose a beam for each UE that maximizes the RSRP while limiting the UE reporting overhead, i.e., we only want the UE to measure the RSRP on a small subset of the available beams before each selection.

Scenario. We assume a BS with M antennas transmitting to a UE with N antennas. Time is slotted and at slot t the channel between the BS and the UE is represented by the matrix $H_t \in \mathbb{C}^{N \times M}$. A set $\Gamma_{\mathrm{BS}} \subset \mathbb{C}^M$ of transmit beams is available to the BS and a *fixed* beam $u \in \mathbb{C}^N$ is used by the UE[1]. If the BS selects beam $b_t \in \Gamma_{\mathrm{BS}}$ and transmits symbol $x_t \in \mathbb{C}$ with power ρ at time t, then the signal received by the UE is,

$$y_t = \sqrt{\rho} u^* H_t b_t x_t + u^* n_t, \tag{1}$$

where $\cdot^*$ and n_t denote the conjugate transpose and the noise term, respectively. Then, we wish to select the beam $b_t \in \Gamma_{\mathrm{BS}}$ for data transmission during the slot t so as to maximize the RSRP $|y_t|^2$. If noise is circular Gaussian this amounts to maximizing $\rho|\bar{H}_t b_t|^2$, where $\bar{H}_t = u^* H_t$ is the channel that the BS perceives, incorporating the UE's beam u.

Ideally, one would want to estimate channel $\bar{H}_t$ and find the element of Γ_{BS} that is closest to the principal eigenvector of $\bar{H}_t^* \bar{H}_t$. However, the feedback required for channel estimation is prohibitive as the number of antennas increases. An alternative is for the BS to choose a set $B_t \subset \Gamma_{\mathrm{BS}}$ of beams and ask the UE to measure the RSRP $|u^* H_t b|^2$ for all $b \in B_t$ and report back each value. Then, the beam $b_t \in \Gamma_{\mathrm{BS}}$ with the highest RSRP is selected for data transmission by the UE during the current slot. Yet, this procedure suffers from high feedback overhead if the UE has to measure a large number of beams. The goal of the *beamtracking* problem that we address in this paper is to select the beam b_t for data transmission

---

[1] The UE usually has a small number of receiving antennas so the constructed receiving beam has a large beam main lobe. Hence, choosing a fixed received beam will not significantly affect the performance

while trading off the achieved RSRP *performance* with the *overhead*, i.e., how many beams the UE measures per slot.

In this work we show how to choose beam b_t via *Bayesian Optimization* (BO). The performance is evaluated according to 1) the *overhead* $|B_t|/|\Gamma_{\mathrm{BS}}|$, 2) the average RSRP *error* $|u^* H_t b_t|^2 / \max_{b \in \Gamma_{\mathrm{BS}}} |u^* H_t b|^2$ and 3) the *accuracy*, i.e., the probability that $|u^* H_t b_t|^2 = \max_{b \in \Gamma_{\mathrm{BS}}} |u^* H_t b|^2$.

A. Related work

The beamtracking literature can be categorized into *i) RSRP-based*—which our contribution belongs to—where the BS determines the best beam for the UE only based on UE RSRP reports, *ii) channel-based*, where the BS is assumed to be able to estimate the channel or at least its covariance matrix, and *iii) side-data assisted*, where additional information is required, such as the GPS position of the UE. Within the *i) RSRP-based* research thread, the work in [4], inspired by [5], relies on the assumption that UE mobility tends to follow repeated patterns, and predicts the best beam for the next slots from previous RSRP measurements via a long short-term memory (LSTM) deep learning architecture. The main bottleneck is the training phase, during which the BS collects a large set of UE reports and trains an LSTM. References [6], [7] predict the beam indexes with highest RSRP as well as blockage events, via deep learning. Similarly to our contribution, the work [8] uses Bayesian Optimization to estimate the best transmit and receive beams. However, the temporal aspect is not studied: once the user moves and/or the channel varies, the optimization has to be repeated from scratch. The *ii) channel-based* thread is arguably the best investigated. The contributions in [9], [10] rely on the assumption that the angles of arrival and departure of the channel evolve according to a Gauss-Markov model, and use a Kalman filter to track the main direction of the channel. The work [11] exploits the ability of HBF transceivers to collect channel information from multiple spatial directions simultaneously, and designs two strategies (exhaustive beam search in a training phase and probabilistic beam tracking) to rapidly estimate the most suitable transmit/receive beams. For this scheme, the training effort is non negligible though. A sub-thread focuses on the assumption that, especially for mmWave, the channel has a sparse representation in the angular domain, i.e., only few scatterers exist. This is exploited by estimating the channel via few linear measurements (which would in turn require the UE to report the complex received signal, instead of the RSRP) and then applying compressed sensing techniques, providing the main angles of arrival and departure of the channel, as in, e.g., [12] and [13]. The *iii) side-data assisted* methods are more common in vehicular-to-infrastructure deployments, where the GPS location of the UE can be used for beamtracking, as in [14], [15], or via computer vision as in [7].

B. DFT Beam Construction

The above problem was defined for an abstract beamset Γ_{BS}, but in practice Γ_{BS} typically consists of an array of 2-dimensional *Discrete Fourier Transform* (DFT) beams. In this configuration the base station has a rectangular $M_H \times M_V$ antenna array with spacing d_H, d_V in the horizontal and vertical directions, respectively. The beamset Γ_{BS} is a collection of DFT beams, defined on a grid of evenly spaced azimuth angles $\{\theta_h\}_{h=1,\ldots,H}$ and elevation angles $\{\phi_v\}_{v=1,\ldots,V}$. The beam $b_{h,v}$ is defined as the following $M_H \times M_V$ matrix:

$$\frac{1}{\sqrt{M_H}} [1, e^{-j 2\pi \frac{d_H}{\lambda} \sin \phi_v \cos \theta_h}, \ldots, e^{-j 2\pi \frac{d_H}{\lambda} (M_H - 1) \sin \phi_v \cos \theta_h}]^T \otimes$$

$$\frac{1}{\sqrt{M_V}} [1, e^{-j 2\pi \frac{d_V}{\lambda} \cos \phi_v}, \ldots, e^{-j 2\pi \frac{d_V}{\lambda} (M_V - 1) \cos \phi_v}], \quad (2)$$

where $j = \sqrt{-1}$, $\otimes$ denotes the Kronecker product and λ is the wavelength. If beam $b_{h,v}$ is selected then the main lobe points in the direction with azimuth/elevation angles θ_h, ϕ_v.

II. BAYESIAN OPTIMIZATION: PRELIMINARIES

Bayesian optimization (BO) is a black-box optimization technique that maximizes an unknown function $f : \mathcal{X} \to \mathbb{R}$, where the domain $\mathcal{X}$ is a metric space, i.e., a (possibly discrete) set endowed with a metric δ. At each iteration i, BO chooses a value of the input variable x_i, observes a (possibly) noisy sample $\widetilde{f}(x_i)$ (also called the *reward*) and updates its estimate of f. BO is *derivative-free* since it is agnostic to the gradient of f and does not attempt to estimate it. BO is especially useful when a near-optimal point needs to be found within a few iterations, due to the expense of evaluating f. We refer to [16] for an in-depth overview of BO. Next we recall its salient features.

Gaussian process. In order to infer the value of the function f at unseen points, BO relies on a statistical model that is typically a Gaussian Process (GP) [17]. Formally speaking, a GP is a collection of random variables, any finite collection of which has a multivariate Gaussian distribution. Hence, to define a GP we require a function defining the mean of each random variable and another function describing the covariance between any pair of variables.

The mean of the GP at each point x is defined via the *prior mean* function $m(.) : \mathcal{X} \to \mathbb{R}$, which provides a reasonable estimation of $f(x)$, prior to any observation. By default, one can set $m(x) = \text{constant}$ for all $x \in \mathcal{X}$. Yet, the choice of an informative prior by, e.g., domain knowledge and/or simulation helps BO to restrict the search region and avoid a cold start.

The covariance between any two elements of the GP is defined via a *kernel* function $k(x, x') : \mathcal{X} \times \mathcal{X} \to \mathbb{R}$. Matérn kernels [17] and the radial basis function (RBF) are classic examples of kernel functions. For instance, the RBF kernel is:

$$k_\theta^{\mathrm{RBF}}(x, x') = \theta_1 \exp\left(\frac{\delta(x, x')}{\theta_2^2}\right), \quad \forall x, x' \in \mathcal{X} \quad (3)$$

where δ is a distance metric and $\theta = [\theta_1, \theta_2]$ is the vector of hyper-parameters. The covariance between $f(x)$ and $f(x')$ is then computed as $\Sigma_{x,x'} = k_\theta(x, x') + \sigma^2 \mathbb{1}(x = x')$, where σ is the standard deviation of the observation noise and $\mathbb{1}(.)$ is the indicator function. The kernel determines the *smoothness* of function f with respect to the metric δ.

BO is an iterative process with three main components. At each iteration we first *infer* the reward at unmeasured points via the GP model. Then, we pick a new point to measure. Finally, we tune the kernel hyper-parameters.

Inference. Until iteration $i - 1$ we have chosen points $\mathbf{x}_{i-1} = \{x_1, \ldots, x_{i-1}\}$ and observed the corresponding rewards $\widetilde{\mathbf{f}}_{i-1} := \{\widetilde{f}(x_1), \ldots, \widetilde{f}(x_{i-1})\}$. At iteration i we want to infer the reward $f(x)$ for *any* point x. By definition of a GP, the random variables $\widetilde{\mathbf{f}}_{i-1}, f(x)$ are jointly Gaussian; moreover, their mean and covariance matrix can be obtained via the prior mean and kernel function, as described above. Therefore, we can infer $f(x)$ from previous measurements via the classic Gaussian posterior probability formula:

$$f(x) \,|\, \widetilde{\mathbf{f}}_{i-1}, \mathbf{x}_{i-1} \sim \mathcal{N}\Big(\mu_x + \Sigma_{x,\mathbf{x}_{i-1}} \Sigma_{\mathbf{x}_{i-1}}^{-1} (\widetilde{\mathbf{r}}_i - \mu_{\mathbf{x}_{i-1}}),$$
$$\Sigma_x - \Sigma_{x,\mathbf{x}_{i-1}} \Sigma_{\mathbf{x}_{i-1}}^{-1} \Sigma_{x,\mathbf{x}_{i-1}}^T\Big) \quad (4)$$

where $\mu_{\mathbf{x}_{i-1}} = [m(x_1), \ldots, m(x_{i-1})]$, $\Sigma_{x,\mathbf{x}_n} = [\Sigma_{x,x_n}]_{1 \leq n < i}$, and $\Sigma_{\mathbf{x}_i} = [\Sigma_{x_n,x_m}]_{1 \leq n,m < i}$.

Choice of next point. Choosing the next point x_i is typically done by maximizing an *acquisition function* a that addresses the following *exploration vs. exploitation* dilemma. On the one hand, we want to exploit the learnings from previous observations and choose x_i where the GP posterior mean is high. On the other hand, to avoid getting stuck in local optima we should explore uncharted regions of $\mathcal{X}$ where the GP standard deviation is high. A well-studied acquisition function is *expected improvement* $a_{\mathrm{EI}}(x)$, computing the expectation of the improvement of the reward upon selecting x with respect to the highest expected reward:

$$a_{\mathrm{EI}}(x) = \mathbb{E}\left[f(x) - \max_{x' \in \mathcal{X}} \mathbb{E}[f(x')]\right]^+, \quad \forall x \in \mathcal{X} \quad (5)$$

where expectations are with respect to the GP posterior.

Hyper-parameters θ, σ can be learned on-the-fly, by maximizing the log-likelihood of the collected reward samples.

The cumulative *regret* of BO (with respect to the oracle solution that chooses the optimal point at all times) grows with the square root of the time horizon, as in [18].

III. BAYESIAN OPTIMIZATION FOR BEAMTRACKING

We now return to our beamtracking problem. We first present our beamset design principles, that we address via BO.

A. Design principles

i) After a UE enters the cell, the BS wants to generate beamsets that can track the high RSRP beams in as few time slots as possible, since beams with low RSRP result in low data rate transmissions for the UE.

ii) The reason we can hope to do effective beamtracking without measuring all beams is that there are correlations in RSRP across the different beams in Γ_{BS} and across time. In particular, as the angular spread of the beams decreases, the RSRP function is increasingly smooth across Γ_{BS}, and as the time slot frequency increases with respect to the channel coherence time, the RSRP function is smoother across time.

iii) The BS needs to determine how many beams should be proposed to the UE at each iteration; as the uncertainty on RSRP decreases, then fewer beams should be used.

Next we show how points i)-iii) can be addressed via BO.

B. Problem formulation via Bayesian optimization

We model the unknown RSRP function for a UE $f_t(b) := |u^* H(t) b|^2$ as a GP whose input variables are $x := (t, b)$, where $t = 0, 1, \ldots$ and $b \in \Gamma_{\mathrm{BS}}$. Here, time $t = 0$ denotes the time that the UE enters the cell served by the BS. As new RSRP measurements are collected over time, we can infer the RSRP offered by a beam at the next iteration via a GP surrogate model, analogous to (4). In particular, we can think of one BO iteration per time slot and so in the sequel we shall use the terms "iteration" and "time slot" interchangeably.

There exist a few twists to the vanilla BO model introduced earlier. First, we have to deal with the augmented time variable t, which we discuss in Section III-C. In particular, at a given time $t = t'$ we can only request measurements of the form $f_{t'}(b)$. Second, we are not simultaneously trying to approximate $f_t(b)$ for all t, b. At time t we are most interested in $f_{t'}(b)$ for t' close to t. Third, we have the freedom to choose *multiple* beams $B \subset \Gamma_{\mathrm{BS}}$ in each time slot, while the acquisition function framework in vanilla BO only caters for a single function evaluation in each iteration. Fourth, we do not simply want to maximize the performance of a beamset in terms of RSRP, but we also wish to limit the associated beam management reporting overhead.

Next we describe our BO approach for beamtracking. We start by defining the kernels, then we construct the prior mean for the GP. Finally, we show how to choose the beamset.

C. Gaussian Process kernel design

The smoothness properties of f, discussed in point ii) above, are captured by the GP kernel $k(\cdot, \cdot)$. It is convenient [19] to decouple the effect of beam and time variables and write the kernel as the product of two independent kernels:

$$k_\theta\big((t, b), (t', b')\big) := k_\theta^{\mathrm{time}}(t, t') \times k_\theta^{\mathrm{beam}}(b, b'). \quad (6)$$

1) Time kernel: The time kernel $k_\theta^{\mathrm{time}}(t, t')$ describes the correlation of two RSRP measurements taken at iterations t and t'. We want our beamtracking method to be applicable to any UE mobility pattern, which we do not even attempt to infer. The most robust choice is then to assume that $k_\theta^{\mathrm{time}}(t, t')$ fades as $|t - t'|$ increases; hence, the time kernel effectively decides the rate at which past samples are forgotten. Our choice for k_θ^{time} is the RBF kernel (cf. Equation 3)

$$k_\theta^{\mathrm{time}}(t, t') := \theta_1 \exp\left(-\frac{t - t'}{\theta_2}\right)^2, \quad \forall\, t, t' \geq 0. \quad (7)$$

where $1/\theta_2$ is the forgetting rate.

2) Beam kernel for DFT beams: To define the beam kernel $k_\theta^{\mathrm{beam}}(b, b')$ one has to first choose the metric δ describing the distance between two beams. We propose here a natural approach based on the definition of DFT beams in Section I-B. Since beams pointing in similar directions are expected to

produce similar RSRP values, it is natural to define the kernel distance δ between two DFT beams $b_{h,v}$ and $b_{h',v'}$ as the weighted Euclidean distance between their indexes:

$$\delta_\ell^{\text{beam}}(b_{h,v}, b_{h',v'}) = \sqrt{(h - h')^2/\ell_H + (v - v')^2/\ell_V} \quad (8)$$

where the weights ℓ_H, ℓ_V account for different spacing in azimuth and elevation of the DFT angle grid. A classic kernel choice [17] is the Matérn kernel $k_\theta^{\text{beam}}(b, b')$, that writes:

$$\frac{1}{\Gamma(\nu)2^{\nu-1}} \left(\sqrt{2\nu}\, \delta_\ell^{\text{beam}}(b, b') \right)^\nu \kappa_\nu \left(\sqrt{2\nu}\, \delta_\ell^{\text{beam}}(b, b') \right) \quad (9)$$

where the kernel hyper-parameters are $\theta = [\nu, \ell_H, \ell_V]$, κ_ν is the modified Bessel function of order ν and Γ denotes the Gamma function. Importantly, the parameter ν controls the smoothness of the learned function.

D. Gaussian process prior mean

We also wish to make use of historical RSRP measurements to restrict the beam search for a new UE when it first connects to the BS. A natural way is to compute the GP prior mean $m_t(b) := m(b)$, $\forall t$ as the average of the RSRP measurements reported by the UEs in the past to the same BS when beam $b \in \Gamma_{\text{BS}}$ was deployed at the BS. This clearly gives a coarse estimation of f, but it can bias the beam search and rule out beams that never worked well in the past (e.g., beams with high elevation degree for the BS in rural areas with UEs located at low altitude). Else, if historical data is not available at the BS, one can set $m_t(b) = \text{constant}$ for all t, b.

E. RSRP Inference

At time t, the BS infers the function $f_t(b)$ for all $b \in \Gamma_{\text{BS}}$ via the GP posterior formula (4), where $x := (t, b)$, with t fixed and beam b ranging over Γ_{BS}, and where past sampling points are $\{(k, b')\}_{k=0,...,t-1, b' \in B_k}$.

F. Beamset optimization via parallel acquisition function

Next, we discuss how the BS chooses the next beamset B_t on which the UE is asked to report RSRP measurements to the BS. First, we assume that the beam b_t used by the UE for data transmission during slot t is the one with highest RSRP among the proposed beamset B_t. We then define accordingly:

$$f_t(B) := \max_{b \in B} f_t(b), \qquad \forall B \subset \Gamma_{\text{BS}}, \ t = 0, 1, \ldots \quad (10)$$

As in the classic BO framework, we choose the *expected improvement* acquisition function (see Equation 5). However, to disincentivize sampling the entire beam dictionary we include a UE feedback overhead, modeled as a convex increasing function $h(.)$ of the beamset cardinality $|B|$, with $h(0) = 0$. Then, the beamset B_t chosen by the BS at time t is given by:

$$B_t = \arg\max_{B \subset \Gamma_{\text{BS}}} \mathbb{E}\left[f_t(B) - f_t^* \right]^+ - h(|B|), \quad (11)$$

where f_t^*, as advocated in [19], is the highest RSRP that is *believed* to be attainable across all beams at time slot t, i.e.,

$$f_t^* := \max_{b \in \Gamma_{\text{BS}}} \mathbb{E}[f_t(b)]. \quad (12)$$

The expression (11) is generally referred to as *parallel BO* [20], where multiple evaluations of the unknown function are possible. To solve the combinatorial problem efficiently a number of approaches are available in the literature, but they either rely on the assumption that observations are sequential [21] (while they occur at adjacent transmission units in our case, hence practically simultaneously from a computation perspective) or that the GP domain $\mathcal{X}$ is continuous [22] (while $\mathcal{X}$ is inherently discrete in our case). Moreover, such approaches are particularly suited when the dimension of $\mathcal{X}$ is large (whereas it is just 2 in the case of DFT beams). Therefore, in the next section we derive an efficient method tailored for our use case that approximates the optimal B_t with low complexity and theoretical guarantees.

1) Greedy algorithm with theoretical guarantees: We now design a method that approximates the optimal B_t with low complexity and theoretical guarantees. Since our analysis holds for any iteration t, we will omit subscript t.

Auxiliary problem. We focus first on a simplified version of problem (11), where the beamset size is fixed and equal to n:

$$J^*(n) = \max_{B \subset \Gamma_{\text{BS}} : |B| = n} J(B) := \mathbb{E}\left[f(B) - f^* \right]^+. \quad (13)$$

We will prove that $J(B)$ is a *monotone* and *submodular* function of the beamset B. Monotonicity states that larger sets bring higher rewards. Submodularity is analogous to concavity and claims that the incremental reward of adding an element to a certain initial set decreases as the initial set enlarges.

Definition 1. *The set-valued function J is* monotone *if $J(\mathcal{B}) \leq J(\mathcal{B}')$, for all $\mathcal{B} \subset \mathcal{B}'$.*

Definition 2. *The set-valued function J is* submodular *if, for all $\mathcal{B} \subset \mathcal{B}'$ and $b^* \notin \mathcal{B}'$, $J(\mathcal{B} \cup b^*) - J(\mathcal{B}) \geq J(\mathcal{B}' \cup b^*) - J(\mathcal{B}')$.*

Proposition 1. *Function $J(.)$ is monotone and submodular.*

Proof: To prove monotonicity we have to show that

$$\mathbb{E}\left[f(B) - f^* \right]^+ \leq \mathbb{E}\left[f(B') - f^* \right]^+, \quad \text{if } B \subset B' \subset \Gamma_{\text{BS}}.$$

This simply stems from the fact that $f(B)$ is the maximum over a set of random variables $\{f(b)\}_{b \in B'}$ that is strictly larger than $\{f(b)\}_{b \in B}$. To prove submodularity we observe that, if $B \subset B'$ and $b^* \notin B'$,

$$[f(B \cup b^*) - f^*]^+ - [f(B) - f^*]^+ \quad (14)$$

$$= [f(b^*) - \max\{f^*, f(b) \ \forall b \in B\}]^+ \quad (15)$$

$$\geq [f(b^*) - \max\{f^*, f(b) \ \forall b \in B'\}]^+ \quad (16)$$

$$= [f(B' \cup b^*) - f^*]^+ - [f(B') - f^*]^+. \quad (17)$$

By taking the expectation of (14),(17) one obtains the submodularity definition of J, q.e.d. ∎

By exploiting a classic result in combinatorial analysis [23] we can claim that a simple greedy algorithm that adds iteratively the beam maximizing the incremental expected improvement (Algorithm 1) achieves an optimality gap of e^{-1}.

Theorem 1. *[23] Let $\underline{J} = \min_{b \in \Gamma_{\text{BS}}} J(\{b\})$. Let $J(B^g(n))$ be the reward achieved by Algorithm 1. Since J is monotone*

and submodular, then the optimality gap is bounded by e^{-1}:

$$\frac{J^*(n) - J(B^g(n))}{J^*(n) - \underline{J}} \le e^{-1} \approx 0.37, \quad \forall n \ge 1. \qquad (18)$$

Algorithm 1: (Auxiliary) Fixed size beamset choice.

---

1 Initialization: Set $B^g(0) := \emptyset$.
2 for $k = 1, \dots, n$ **do**
3   Compute
         $b^g(k) := \arg\max_{b \in \Gamma_{BS} \setminus B^g(k-1)} J(B^g(k-1) \cup b)$
4   Set $B^g(k) := B^g(k-1) \cup b^g(k)$
5 return beamset $B^g(n)$

Optimized beamset. We can now finally address our original problem in (11), where the beamset size is *not* fixed. In principle, one could run Algorithm 1 for all n's and then choose the beamset $B^g(\bar{n})$ with highest objective $J(B^g(\bar{n})) - h(\bar{n})$, for some $\bar{n} \ge 1$. Yet, recomputing the optimized beamset $B^g(n)$ from scratch for every n is redundant: the iterative nature of greedy Algorithm 1 suggests that, once $B^g(n)$ is computed, one only has to add $b^g(n+1)$ to obtain $B^g(n+1)$. Moreover, it is not necessary to add beams indefinitely, but only until a limited size. To show this, we first observe that $J(B^g(n))$ is the discrete version of a concave increasing function.

Fact 1. *The function $J(B^g(n))$ is increasing in n, while its increments are decreasing in n, i.e., for all $n > 1$, i.e., $J(B^g(n+1)) - J(B^g(n)) \le J(B^g(n)) - J(B^g(n-1))$.*

The difference between a concave increasing function (J) and a convex increasing function (h) has at most one inflection point. Thus, to approximate the beamset selection problem (11) it suffices to add beams iteratively as in greedy Algorithm 1, until the objective function $J(B^g(n)) - h(n)$ starts decreasing. We recap this procedure in Algorithm 2, used by the BS to compute at each time slot t the beamset B_t.

Algorithm 2: Choice of beamset B_t at time slot $t \ge 0$

---

1 Goal: maximize expected improvement as in (11).
2 Initialization: Set $B^g(1) := \arg\max_{b \in \Gamma_{BS}} J(b)$.
3 for $n = 2, 3, \dots$ **do**
4   Compute
         $b^g(n) = \arg\max_{b \in \Gamma_{BS} \setminus B^g(n-1)} J(B^g(n-1) \cup b)$
5   Set $B^g(n) := B^g(n-1) \cup b^g(n)$
6   **if** $J(B^g(n)) - h(n) \le J(B^g(n-1)) - h(n-1)$ **then**
7   **return** beamset $B_t = B^g(n-1)$.
8 BS proposes beamset B_t to the UE at time slot t.

Practical implementation of Algorithm 2. A closed formula for $J(B)$ is only known for $|B| = 1, 2$ (see [17], [21], respectively). Hence, in practice, $J(B)$ should be estimated via Monte-Carlo sampling from the GP posterior distribution for $|B| \ge 3$. To further reduce complexity, efficient sampling methods with linear complexity in the number of observations can be used, such as the one in [24].
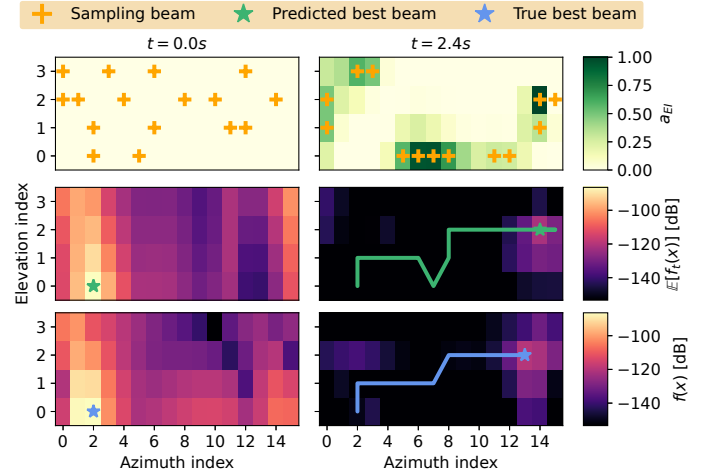

Fig. 1. Time history of a typical UE at time slots $0, 30$. Top row: Acquisition function (Expected Improvement) used to choose sample beam indices (orange crosses). Center row: Posterior mean with predicted best beam index (green star) and path trace (green line) overlaid. Bottom row: True RSRP landscape with true best beam (blue star) and path trace (blue line) overlaid.

Algorithm 3: BO for beamtracking

---

1 Initialization. Choose the kernel function k_θ as the product of beam and time kernels as in Sect. III-C;
2 BS computes the prior mean m as in Sect. III-D;
3 BS initializes the hyper-parameters θ, σ;
4 UE connects to BS at time $t = 0$.
5 for *time slot* $t = 0, 1, \dots$ **do**
6   BS computes the beamset B_t via Algorithm 2;
7   UE reports the RSRP for each beam in B_t;
8   BS uses beam $b_t \in B_t$ with highest reported RSRP for data transmission to the UE until next slot;
9   BS updates θ, σ via max-likelihood;
10 end

For the reader's convenience, in Algorithm 3 we recap the main steps of our BO algorithm for beamtracking. In Figure 1 we provide a typical UE time history visualizing the 2D acquisition function, posterior distribution, and ground truth.

IV. NUMERICAL RESULTS

We evaluate our approach using a 5G NR 3GPP-compliant system level simulator and benchmark its performance against single-slot (spatial) algorithms that only use RSRP information from the current timeslot and an LSTM-based multi-slot (spatio-temporal) algorithm that (like BO) also utilizes past measurements. In out BO setup we use a non-informative prior mean function (i.e., $m_t(b) = 0$ for all $t, b \in \Gamma_{BS}$), mimicking execution at the BS without any offline training or *a priori* tuning. The simulation specifications are found in Table I.

We first compare our method to two spatial interpolation approaches: a Scipy implementation of (rectilinear bivariate) spline interpolation [25], and a Scikit-Learn implementation of Gaussian process regression [26] with a Matérn 3/2 kernel. For these interpolation methods, we first sample a subset of beams $B_\phi \subset \Gamma_{BS}$ where the subscript ϕ denotes the

Scenario	3D-UMi-street Canyon
Deployment	Hexagonal grid, 7 BS sites, 21 cells,
	BS antenna height 10m (downtilt $10°$)
ISD	100m
Carrier	28 GHz
Bandwidth	50 MHz
Spacing	120 kHz
Frame	TDD, DL data frame only
gNB antenna	(M, N, P, Mg, Ng) = (16, 16, 2, 1, 1)
	dual-polarized panel arrays
gNB GoB	64 Tx beams: Tx Beam Azimuth (deg)
	$= -56.25 + 7.5n$, $n = 0, \ldots, 15$
	Elevation (deg) = $\{0, 7.5, 15, 22.5\}$
UE antenna	(M, N, P) = (2, 2, 2) per dual-polarized panel
	UE orientation uniformly distributed
HARQ	No retransmission
Traffic Models	Traffic model: full buffer
UE distribution	10 UEs/sector, randomly distributed
	100% of UEs outdoor
UE speed	30, 45, 60, 75, 90 km/h
Time slot	80ms
UE trajectory	Straight with random direction
Channel	3GPP spatial consistency with proc. A

Fig. 2. Left column: Bayesian optimization (low overhead configuration) evolution of accuracy, overhead, and RSRP error for varying UE speeds. Right column: PredRNN ($(J, K) = (5, 15)$ configuration) evolution of accuracy, overhead, and *RSRP* error for varying UE speeds.

proportion of Γ_{BS}, and choose the best beam b_t according to $\arg\max_{b \in B_\phi} \text{RSRP}(b)$. We consider two sampling fractions: $\phi \in \{0.25, 0.5\}$. For our BO method, we consider two setups: a *high accuracy* configuration prioritizing accuracy by allowing for a larger sampling beamset cardinality and encouraging more exploration by reducing the overhead penalty function $h(.)$; a *low overhead* configuration prioritizing overhead by restricting the beamset cardinality to be at most 16 (i.e. 12.5% of the 64 available beams in Γ_{BS}) and increasing the penalty function $h(.)$, thereby making the sampling more greedy.

The performance of all schemes for 3 different UE speeds is shown in Table II. Here, RSRP error is measured in dB. Gaussian process regression (GPR) requires a sampling fraction of 0.5 to achieve acceptable accuracy and RSRP error, although this error is above 1 dB across all speeds even with a sampling fraction of 0.5. Of these two interpolation methods, spline interpolation performs the best across all three metrics, which is notable since it has a lower computational complexity.

The high accuracy BO method achieves over 90% accuracy and sub 1 dB RSRP error with an overhead around 20% across all speeds tested. Only spline interpolation achieves marginally higher accuracy and lower RSRP error at a UE speed of 90 km/h, albeit with over double the overhead. Even with an overhead of only 12%, the low overhead BO method is able to achieve approximately 90% accuracy and 1 dB RSRP error at UE speeds lower than 60 km/h.

Finally, we compare our BO method for beamtracking to a spatio-temporal algorithm described in [27] that utilizes a reimplementation of PredRNN, a recurrent neural network for predictive learning using Long Short-Term Memory (LSTM) units [28]. PredRNN uses a so-called unified memory pool, allowing the spatio-temporal LSTM units to extract both spatial and temporal representations simultaneously. We refer to [28] for full details. PredRNN [27] predicts the *most probable*
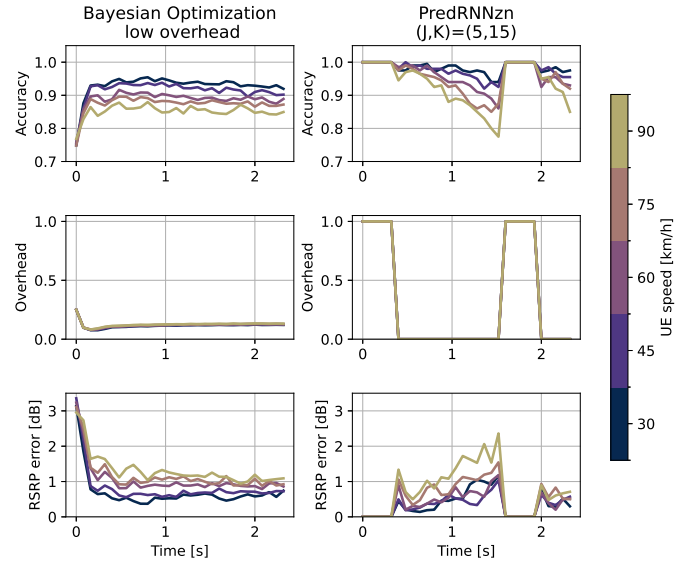
length-K sequence of best beams b^* given the previous length-J sequence including the current observation:

$$b^*_{t+1}, \ldots, b^*_{t+K} = \arg\max_{b_{t+1}, \ldots, b_{t+K}} p\left(b_{t+1}, \ldots b_{t+K} | b^*_{t-J+1}, \ldots b^*_t\right).$$

Given that PredRNN requires noiseless inputs, we sample *all* beam indexes for J time slots and then predict the next K time slots, repeating this sampling/prediction cycle until the UE has left the domain. In Table II we show performance for $(J, K) = (5, 5)$ (i.e., $\phi = 0.5$) and for $(J, K) = (5, 15)$ (i.e., $\phi = 0.25$). PredRNN typically achieves high accuracy and low RSRP error when the overhead is 0.5 (which is higher overhead than for the BO methods), but the accuracy and RSRP error deteriorate as we lower the overhead to 0.25.

Figure 2 shows the evolution of accuracy, overhead, and RSRP error for both BO and PredRNN (left and right columns, respectively). For our BO-based approach, accuracy and RSRP error degrade with increasing UE speed, as seen in Table II. Interestingly, the accuracy and RSRP error improve approximately monotonically, while there is a distinct undershoot in the overhead metric near $t \approx 0.3$ before converging towards approximately 12.5% (or 20% for the high accuracy configuration). We attribute this undershoot to the development of the time kernel during the cold-start: without *a priori* knowledge the RSRP landscape is initially treated as static (with a large temporal length scale), but as RSRP measurements come in temporal correlations become apparent, driving the temporal length scale down. The shift from static to dynamic RSRP landscape manifests itself in a broadening of the posterior, promoting more exploration and an increase in the overhead.

For PredRNN, the overhead is at 100% during the training phase and then comes down to 0% during the prediction phase. The accuracy and RSRP error start to deteriorate as soon as we

		$s = 30\,\text{km/h}$			$s = 60\,\text{km/h}$			$s = 90\,\text{km/h}$		
		Accuracy	Overhead	RSRP error	Accuracy	Overhead	RSRP error	Accuracy	Overhead	RSRP error
Spline	$\phi = 0.25$	0.804	0.25	2.36	0.781	0.25	2.35	0.770	0.25	2.37
	$\phi = 0.5$	0.934	0.5	0.653	0.926	0.5	0.639	0.916	0.5	0.669
GPR	$\phi = 0.25$	0.329	0.25	13.1	0.353	0.25	12.0	0.361	0.25	11.3
	$\phi = 0.5$	0.885	0.5	1.21	0.880	0.5	1.14	0.872	0.5	1.11
PredRNN	$(J, K) = (5, 5)$	0.933	0.5	0.217	0.924	0.5	0.294	0.903	0.5	0.507
	$(J, K) = (5, 15)$	0.891	0.25	0.465	0.873	0.25	0.705	0.815	0.25	1.66
BayesOpt	low overhead	0.943	0.116	0.627	0.900	0.122	1.05	0.874	0.126	1.23
	high accuracy	0.961	0.195	0.425	0.931	0.207	0.700	0.908	0.21	0.929

enter the prediction phase, especially for the higher UE speeds. This is in contrast to our BO-based method, which after the cold-start, displays consistent performance over the remaining slots. A major difference between our BO-based method and PredRNN is that the latter requires offline training whereas the BO results in this section are obtained entirely online with *no pretraining*–although in principle BO can leverage historical data to train its prior mean, as discussed in Section III-D.

V. CONCLUSIONS

In this paper we have described how Bayesian Optimization (BO) provides an effective paradigm for beamtracking so that the UE can maintain connection to a high-RSRP beam by measuring a limited set of beams in every time slot. There are multiple ways in which this work can be extended. First, if the beam dictionary is more exotic than classic DFT then the kernel choice is less evident. One could use *meta-learning* techniques [29] where the metric δ computing the distance between points in $\mathcal{X}$ is defined by a neural network. Second, one could extend our approach by concurrently scheduling wide and narrow beams, to achieve increased flexibility and reduced overhead with respect to the standard hierarchical wide (SSB) and narrow (CSI-RS) beam selection in 5G.

REFERENCES

[1] Z. Pi and F. Khan, "An introduction to millimeter-wave mobile broadband systems," *IEEE comm. mag.*, vol. 49, no. 6, pp. 101–107, 2011.

[2] R. W. Heath *et al.*, "An overview of signal processing techniques for millimeter wave MIMO systems," *IEEE journal of selected topics in signal processing*, vol. 10, no. 3, pp. 436–453, 2016.

[3] M. Giordani, M. Polese, A. Roy, D. Castor, and M. Zorzi, "A tutorial on beam management for 3GPP NR at mmWave frequencies," *IEEE Communications Surveys & Tutorials*, vol. 21, no. 1, pp. 173–196, 2018.

[4] A. Ö. Kaya and H. Viswanathan, "Deep learning-based predictive beam management for 5G mmwave systems," in *2021 IEEE Wireless Communications and Networking Conference (WCNC)*, 2021, pp. 1–7.

[5] A. Alahi *et al.*, "Social LSTM: Human trajectory prediction in crowded spaces," in *IEEE CVPR*, 2016, pp. 961–971.

[6] F. Göttsch and M. Kaneko, "Deep Learning-based Beamforming and Blockage Prediction for Sub-6GHz/mm Wave Mobile Networks," in *IEEE GLOBECOM 2020*, 2020, pp. 1–6.

[7] T. Nishio, Y. Koda, J. Park, M. Bennis, and K. Doppler, "When wireless communications meet computer vision in beyond 5G," *IEEE Communications Standards Magazine*, vol. 5, no. 2, pp. 76–83, 2021.

[8] S. Yang, B. Liu, Z. Hong, and Z. Zhang, "Bayesian Optimization-Based Beam Alignment for MmWave MIMO Communication Systems," in *2022 IEEE PIMRC*. IEEE, 2022, pp. 825–830.

[9] V. Va, H. Vikalo, and R. W. Heath, "Beam tracking for mobile millimeter wave communication systems," in *IEEE GlobalSIP*, 2016, pp. 743–747.

[10] X. Xin and Y. Yang, "Robust Beam Tracking with Extended Kalman Filtering for Mobile Millimeter Wave Communications," in *2019 IEEE ComComAp*, 2019, pp. 172–177.

[11] J. Palacios, D. De Donno, and J. Widmer, "Tracking mm-Wave channel dynamics: Fast beam training strategies under mobility," in *IEEE INFOCOM 2017*, 2017, pp. 1–9.

[12] T.-H. Chou, N. Michelusi, D. J. Love, and J. V. Krogmeier, "Wideband Millimeter-Wave Massive MIMO Channel Training via Compressed Sensing," in *2021 IEEE GLOBECOM*, 2021, pp. 1–6.

[13] E. Khordad, I. B. Collings, and S. V. Hanly, "A Kronecker-based sparse compressive sensing matrix for millimeter wave beam alignment," in *2019 ICSPCS*, 2019, pp. 1–5.

[14] V. Va, J. Choi, T. Shimizu, G. Bansal, and R. W. Heath, "Inverse multipath fingerprinting for millimeter wave V2I beam alignment," *IEEE Trans. on Vehicular Technology*, vol. 67, no. 5, pp. 4042–4058, 2017.

[15] V. Va, T. Shimizu, G. Bansal, and R. W. Heath, "Online learning for position-aided millimeter wave beam training," *IEEE Access*, vol. 7, pp. 30 507–30 526, 2019.

[16] B. Shahriari, K. Swersky, Z. Wang, R. P. Adams, and N. De Freitas, "Taking the human out of the loop: A review of Bayesian optimization," *Proceedings of the IEEE*, vol. 104, no. 1, pp. 148–175, 2015.

[17] C. K. Williams and C. E. Rasmussen, *Gaussian processes for machine learning*. MIT press Cambridge, MA, 2006, vol. 2, no. 3.

[18] N. Srinivas, A. Krause, S. M. Kakade, and M. W. Seeger, "Gaussian process optimization in the bandit setting: No regret and experimental design," in *Proceedings of ICML-10*, 2010, pp. 1015–1022.

[19] J. Richter, J. Shi, J.-J. Chen, J. Rahnenführer, and M. Lang, "Model-based optimization with concept drifts," in *Proceedings of the 2020 genetic and evolutionary computation conference*, 2020, pp. 877–885.

[20] P. I. Frazier, "A tutorial on Bayesian optimization," *arXiv preprint arXiv:1807.02811*, 2018.

[21] D. Ginsbourger, R. L. Riche, and L. Carraro, "Kriging is well-suited to parallelize optimization," in *Computational intelligence in expensive optimization problems*. Springer, 2010, pp. 131–162.

[22] J. Wang, S. C. Clark, E. Liu, and P. I. Frazier, "Parallel Bayesian global optimization of expensive functions," *Operations Research*, vol. 68, no. 6, pp. 1850–1865, 2020.

[23] G. L. Nemhauser, L. A. Wolsey, and M. L. Fisher, "An analysis of approximations for maximizing submodular set functions—i," *Mathematical programming*, vol. 14, no. 1, pp. 265–294, 1978.

[24] J. Wilson *et al.*, "Efficiently sampling functions from Gaussian process posteriors," in *International Conference on Machine Learning*. PMLR, 2020, pp. 10 292–10 302.

[25] P. Virtanen *et al.*, "SciPy 1.0: Fundamental Algorithms for Scientific Computing in Python," *Nature Methods*, vol. 17, pp. 261–272, 2020.

[26] F. Pedregosa *et al.*, "Scikit-learn: Machine learning in Python," *Journal of Machine Learning Research*, vol. 12, pp. 2825–2830, 2011.

[27] Nokia, "Other aspects on ML for beam management." [Online]. Available: https://www.3gpp.org/ftp/TSG_RAN/WG1_RL1/TSGR1_109-e/Docs/R1-2204574.zip

[28] Y. Wang *et al.*, "PredRNN: Recurrent Neural Networks for Predictive Learning using Spatiotemporal LSTMs," in *Advances in Neural Information Processing Systems*, vol. 30. Curran Associates, Inc., 2017.

[29] J. Rothfuss, V. Fortuin, M. Josifoski, and A. Krause, "PACOH: Bayes-optimal meta-learning with PAC-guarantees," in *International Conference on Machine Learning*. PMLR, 2021, pp. 9116–9126.